



This is a repository copy of *Acritarch Palynomorph Darkness Index (PDI) as an indicator of thermal maturity in Silurian sections from Saudi Arabia*.

White Rose Research Online URL for this paper:

<https://eprints.whiterose.ac.uk/219349/>

Version: Published Version

Article:

Clayton, G., Vecoli, M., Luo, P. et al. (2 more authors) (2024) Acritarch Palynomorph Darkness Index (PDI) as an indicator of thermal maturity in Silurian sections from Saudi Arabia. *Marine and Petroleum Geology*, 169. 107049. ISSN 0264-8172

<https://doi.org/10.1016/j.marpetgeo.2024.107049>

Reuse

This article is distributed under the terms of the Creative Commons Attribution (CC BY) licence. This licence allows you to distribute, remix, tweak, and build upon the work, even commercially, as long as you credit the authors for the original work. More information and the full terms of the licence here:

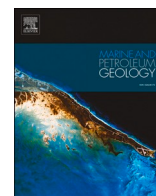
<https://creativecommons.org/licenses/>

Takedown

If you consider content in White Rose Research Online to be in breach of UK law, please notify us by emailing eprints@whiterose.ac.uk including the URL of the record and the reason for the withdrawal request.



eprints@whiterose.ac.uk
<https://eprints.whiterose.ac.uk/>



Acritarch Palynomorph Darkness Index (PDI) as an indicator of thermal maturity in Silurian sections from Saudi Arabia

Geoff Clayton^{a,*}, Marco Vecoli^b, Pan Luo^c, Robbie Goodhue^d, Charles Wellman^a

^a School of Biosciences, University of Sheffield, Sheffield, S10 2TN, UK

^b Saudi Aramco, Dhahran, Saudi Arabia

^c EXPEC Advanced Research Center, Saudi Aramco, Dhahran, Saudi Arabia

^d Department of Geology, Trinity College, University of Dublin, Dublin D02 PN40, Ireland

ARTICLE INFO

Keywords:

Acritarchs

PDI

Fluorescence

Qusaiba member

Qalibah formation

Silurian

Hot shales

Thermal maturity

ABSTRACT

Palynomorph Darkness Index (PDI) measurements on acritarchs from Silurian strata in Saudi Arabia exhibit an irregular but potentially useful relationship to other vitrinite reflectance proxies. Four distinct stages in PDI evolution can be recognized with thermal maturity. In Stage 1, acritarch PDI is <10% and shows no increase with increasing maturity. A very rapid increase in PDI towards the end of the oil window from <10% to ca. 25% characterises Stage 2, which is followed by a gradual increase in Stage 3 from ca. 25% to approximately 80%. PDI Stage 4 is represented by postmature rocks, with acritarch PDI >82% and showing little change with increasing maturity. Acritarch fluorescence is totally extinguished within the oil window.

1. Introduction

1.1. Geological setting

During the early Silurian, widespread deposition of organic-rich shales occurred across the northern margin of Gondwana, including North Africa and the Arabian Peninsula (Lüning et al., 2000; Loydell et al., 2009, 2013). The deposition and stratigraphic development of these sediments have been associated with the post-glacial paleoenvironmental conditions during and following the melting of the Late Ordovician ice cap, which directly influenced paleotopography, eustatic variations, sediment input, and depositional patterns (Lüning et al., 2000; Hayton et al., 2017; Vecoli et al., 2011). According to Lüning et al. (2000), the lower Silurian shales, especially the characteristic basal organic-rich (“hot”) shale units, are at the origin of the vast majority of the Palaeozoic-sourced hydrocarbons in North Africa and the Middle East.

In Saudi Arabia, early Silurian deposits are represented within the predominantly shaly Qusaiba Member (abbreviated to QMbr herein), which is the basal unit of the Qalibah Formation (Fig. 1; Hayton et al., 2017). The QMbr rests disconformably on the glaciogenic,

predominantly sandy Sarah Formation and is in diachronous contact with the overlying, predominantly sandy Sharawra Member, representing the upper unit of the Qalibah Formation (Fig. 1). The Palaeozoic palyno- and biostratigraphy Saudi Arabia was reviewed by Wellman et al. (2015).

Especially in its lower part, the QMbr contains a series of distinct intervals characterized by high-TOC “warm” and “hot shale” facies, including the widespread basal Silurian hot shales (Base Qusaiba Hot Shale) which have high petroleum generation potential (Cole et al., 1994; Hayton et al., 2017). Additionally, their unusually high organic content makes the Qusaiba shales an important target for unconventional hydrocarbon exploration (Inan et al., 2016). The age of the Qusaiba organic-rich intervals has been established as Rhuddanian to Telychian, based on an integrated (palynological and graptolite) high-resolution biozonation developed for the QMbr (Boukhamsin et al., 2013; Williams et al., 2016; Hayton et al., 2017).

In contrast to its stratigraphic position, the thermal maturity of the QMbr has proved difficult to establish consistently due to the absence of vitrinite, with Tmax- and graptolite reflectance-based “Vitrinite Reflectance Equivalents” (VREs) amongst the most extensively used methods (Cole, 1994; Inan et al., 2016). Multiple methods, including

* Corresponding author.

E-mail addresses: g.clayton@sheffield.ac.uk (G. Clayton), marco.vecoli@aramco.com (M. Vecoli), pan.luo@aramco.com (P. Luo), goodhue@tcd.ie (R. Goodhue), c.wellman@sheffield.ac.uk (C. Wellman).

<https://doi.org/10.1016/j.marpetgeo.2024.107049>

Received 30 April 2024; Received in revised form 7 August 2024; Accepted 8 August 2024

Available online 15 August 2024

0264-8172/© 2024 The Authors. Published by Elsevier Ltd. This is an open access article under the CC BY license (<http://creativecommons.org/licenses/by/4.0/>).



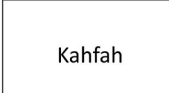
SYSTEM / PERIOD	SERIES / EPOCH	STAGE / AGE	LITHOSTRATIGRAPHY		
			FORMATION	MEMBER	
SILURIAN*	PRIDOLI		TAWIL*	Middle*	
		LUDLOW		Ludfordian	Lower
	WENLOCK	Gorstian	QALIBAH		
		Homerian			
		Sheinwoodian			
	LLANDOVERY	Telychian	QUSAIBA		
		Aeronian			
		Rhuddanian			
	ORDOVICIAN*	UPPER	Hirnantian	SARAH	Quwarah
			Katian		Ra'an
Sandbian			QASIM		Kahfah
					Hanadir
MIDDLE*		Darriwillian*			

Fig. 1. Stratigraphic setting of the QMbr (Qalibah Formation). * = in part.

biomarker ratios, organic petrography, and optical spectroscopy were attempted recently to assess the thermal maturity of the QMbr (Inan et al., 2016; Cheshire et al., 2017; Ertug et al., 2019). However, these methods (except Tmax) are time consuming and still demonstrated large uncertainties for high maturity samples. Another method that could be employed is chitinozoan reflectance, as described by Tricker (1992), which increases in a linear manner with increasing maturity through the oil window. However, this technique has not been widely employed, possibly due to the perception that sample preparation, suitable particle identification and reflectance measurement are relatively complex.

The present study utilized existing Tmax and graptolite reflectance datasets to calibrate acritarch Palynomorph Darkness Index (PDI) results, in order to assess the usefulness of PDI as a proxy for thermal maturity. The aim of the study is to develop a quick and reliable PDI method to estimate thermal maturity and provide a new VRE for an integrative maturity assessment on important hydrocarbon source rocks and unconventional reservoirs.

1.2. Previous work

1.2.1. Vitrinite reflectance equivalents (VREs)

Vitrinite reflectance (VR_o) is the standard oil industry method for estimating thermal maturity but plants producing woody tissues (the precursors of vitrinite) did not evolve until Early Devonian time (Strullu-Derrien et al., 2019), so VR_o cannot be determined in rocks older than this. Many proxies for VR_o , known as Vitrinite Reflectance Equivalents (VREs) have been developed for rocks lacking suitable vitrinite for VR_o measurement, some of the most widely used of which are based on Tmax measurements obtained from pyrolysis. It is convenient and fast to measure Tmax via temperature programmed pyrolysis on

source rock samples. The advantages and pitfalls of this simple maturity proxy were comprehensively reviewed by Yang and Horsfield (2020). In the case of QMbr in Saudi Arabia, there are four challenges in the use of Tmax.

- (1) dry gas window and overmature samples present an extremely low S2 yield or even an undetermined S2 peak in the pyrolysis, which results in significant uncertainty for maturity assessment of high maturity samples;
- (2) the carryover effect of S1 (free hydrocarbon) on the S2 (generatable hydrocarbon) by the use of oil-based mud while drilling in the shale formation may reduce Tmax values and underestimate the maturity.
- (3) suppression of Tmax (abnormally low) has been observed for the QMbr hot shale (very high TOC).
- (4) solid bitumen and pyrobitumen in source rocks may interfere with the S2 peak with multi-modal patterns presenting in temperature programmed pyrolysis, thus producing anomalous Tmax results.

Numerous Tmax to VR_o conversion equations have been established but discussion of these is limited here to the three most relevant versions.

1. Jarvie et al. (2001). This (VRE_J) was one of the first used Tmax correlations to VR_o for Type II kerogen, which was established based on the data of Barnett shale. It is probably still the most extensively used.
2. Inan et al. (2016). The correlation presented by these authors (VRE_I) was based on a wide-ranging investigation of the maturity of QMbr hot shales from Saudi Arabia. Results from numerous analytical methods were utilized, including graptolite reflectance, FTIR spectroscopy, Raman spectroscopy and UV fluorescence.
3. Evenick (2021). This author analyzed a very large dataset comprising 33,732 Tmax and approximately coincident VR_o measurements. This research documented a positive correlation between Tmax and VR_o (VRE_E) but noted considerable scatter in the data, with a trendline equation of, $VR_o = (0.013 \times Tmax) - 5.0$, and an R^2 value of only 0.22. It is also noteworthy that Tmax-derived thermal maturity estimates are most reliable between the values of 430 °C and 500 °C and that Tmax to VR_o correlations significantly weaken at the beginning of the dry gas window (VR_o 1.5%).

1.2.2. Palynomorph colour

The first widely used colour scale, named the 'Thermal Alteration Index (TAI) was published by Staplin (1969). Initially, this was intended to be applied to all "organic debris" from samples examined in transmitted light but it was rapidly refined by being restricted to spores and pollen. The TAI scheme was soon superseded by the 'Spore Colour Index' (SCI) published by Collins (1990) and subsequently refined by Collins and other authors. Attempts have been made to correlate colour classes in the TAI and SCI scales to VR_o (e.g., Ertug et al., 2019) but the fact remains that the TAI and SCI colour class numbers are simply labels, not measurements and that these are not quantitative schemes.

Attempts to fully quantify palynomorph colour include Marshall (1991) and Milton (1993). These authors used micro-spectrophotometry to characterise spore colour, expressing their results in terms of the Commission Internationale de l'Eclairage (CIE) colour system. As noted by Hartkopf-Fröder (2015), micro-spectrophotometry equipment is expensive and only available in few specialist laboratories but it is the method of choice when quantitative and reproducible miospore colour data are needed.

Yule et al. (1998) established a method of quantitative spore colour measurement using colour image analysis (CIA) which they calibrated against VR_o from the same, naturally matured Carboniferous samples. These authors noted a rapid change in quantitative spore colour in the

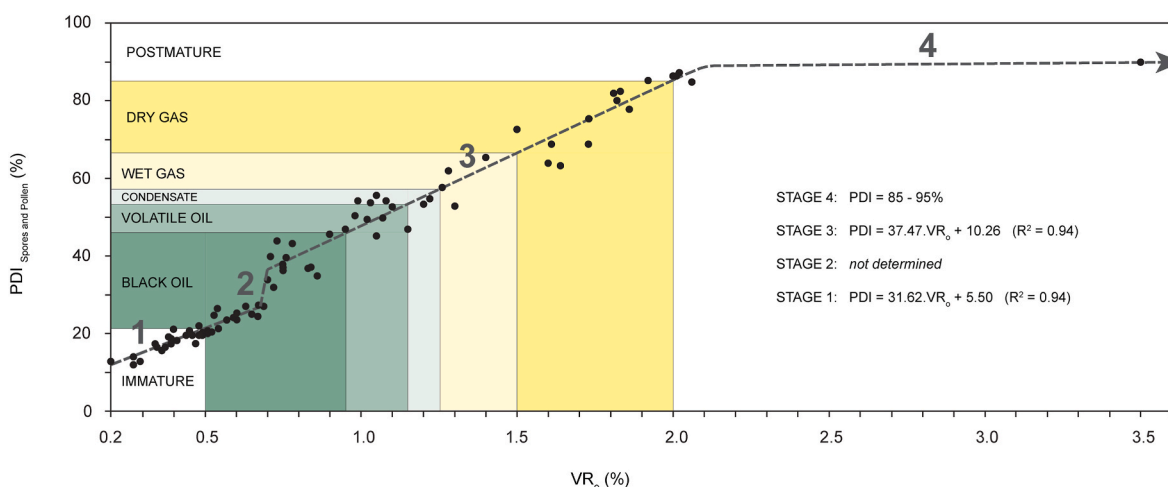


Fig. 2. Correlation of PDI_{Spores and Pollen} to measured VR_o modified from Buratti et al. (2024). The black arrow denotes more data points not included in the figure.

interval VR_o 0.6–1.04%, with the greatest range of colour in a single sample also recorded within this maturity interval.

1.2.3. Acritarch colour

Williams et al. (1998) published a ‘Thermal Alteration Index of Acritarchs’ (Acritarch Alteration Index, AAI) scheme based on visually estimated acritarch colours in transmitted light together with fluorescence. This scheme was tentatively correlated to VR via graptolite reflectance determinations from the Lower Palaeozoic sections and (measured) VR determined from overlying Devonian and Carboniferous rocks. The assumption of these authors that graptolite reflectance could be substituted for VR subsequently proved inaccurate, with Goodarzi et al. (1992) suggesting that the relationship of graptolite reflectance-based VRE (VRE_G) to GR_o could be expressed by VRE_G = 0.80 x GR_o, and Petersen et al. (2013) concluding that VRE_G = (0.73 x GR_o) + 0.16. It also became apparent that graptolites, like vitrinite, are anisotropic, leading to strong bireflectance at high levels of maturity and consequent errors if mean rather than maximum GR_o is used to estimate maturity. A comprehensive review of graptolite reflectance is included in Hartkopf-Fröder (2015). Despite this later work proving some of their interpretations incorrect, Williams et al. (1998) made some important observations, notably that acritarch colour and fluorescence (AAI) change rapidly through the middle part of the oil window.

Duggan and Clayton (2008) measured red, green and blue (RGB) intensities of white light transmitted through acritarchs (*Veryhachium*

spp.) and correlated the values obtained to VR_o measured from the same Silurian – Devonian samples. The relatively poor correlation of RGB intensities to VR_o in this study are probably explained by very small vitrinite-like organic particles in the Silurian samples having the same reflectance as vitrinite, and to inadequate stabilisation of the background light intensity.

1.2.4. Acritarch fluorescence

Spore and pollen fluorescence have been used in several studies to characterise thermal maturity and to discriminate between different palynomorph types. These have been comprehensively reviewed by McPhilemy (1998), Teichmüller and Wolf (1977) and Van Gijzel (1967). Fluorescence of Ordovician palynomorphs from Estonia was correlated to other maturity indicators, including Acritarch Alteration Index, Palynomorph Darkness Index and organoclast reflectance by Sorci et al. (2020).

1.2.5. Palynomorph Darkness index (PDI)

Palynomorph Darkness Index (PDI) is a fully quantitative thermal maturity indicator established by Goodhue and Clayton (2010) based on measurement of the red, green and blue intensities of white light transmitted through palynomorphs. Several accounts of correlation of spore and pollen PDI to VR_o determined from the same samples have been published, including Clayton et al. (2017), Spina et al. (2018) and Spina et al. (2021). Buratti et al. (2024) presented a correlation of spore

VRE _j (%)	HYDROCARBONS	WELL SECTIONS STUDIED (CORE)							
0.50	IMMATURE	869-3	616-5	242-3					
0.95	BLACK OIL				403-3	895-3	853-3	488-31-1	
1.15	VOLATILE OIL	786-3	667-53A						
1.25	CONDENSATE								
1.50	WET GAS	667-165	807-3	667-47	868-3				
	DRY GAS					326-3	854-3-1		

Fig. 3. Well sections of QMbr investigated ranked in order of thermal maturity estimated by VRE_j. No scale implied.

Table 1

All QMbr data. PDI results determined independently by a second operator are shown in bold italics. Samples 20-24 from the QMBr lower hot shale may have been affected by Tmax suppression.

Well	Sample Number	Total Organic Carbon (TOC) (%)	Hydrogen Index (HI) (mg HC/g TOC)	VRE _J (%)	VRE _I (%)	VRE _G (%)	Hydrocarbon Source Rock Interpretation	Veryhachium/Neoverhachium Group				All Acritarchs			
								PDI _V (%)	Standard Deviation	Number of Specimens	Fluorescence	PDI _A (%)	Standard Deviation	Number of Specimens	Fluorescence
616-5	1	0.6	155	0.60	0.80		Immature/Black Oil	2	2	30		3	3	30	Y
	2	6.6	428	0.76	0.93		Black Oil	6	2	30	Y	5	2	30	Y
869-3	3	3.3	432	0.47	0.71		Immature	5	2	30	Y	6	3	30	Y
242-3	4	0.9	93	0.58	0.79		Immature/Black Oil	4	1	30	Y	5	3	30	Y
	5	0.5	182	0.58	0.79		Immature/Black Oil	5	3	30	Y	5	2	30	Y
403-3	6	0.6	147	0.67	0.86		Black Oil	5	2	30	Y	5	2	30	Y
	7	0.5	136	0.71	0.89		Black Oil	6	3	30	Y	5	2	30	Y
895-3	8	0.5	199	0.74	0.91		Black Oil	5	2	30	Y	5	2	30	Y
	9	2.1	352	0.85	0.99		Black Oil	20	7	30	DY	14	9	30	DY
853-3	10	0.6	155	0.76	0.93		Black Oil	5	4	30	DY	5	4	30	DY
	11	0.5	142	0.77	0.93		Black Oil	6	4	30	DY	5	4	30	DY
488-31-1	12	3.9	378	0.80	0.95		Black Oil	6	3	30	DY	6	2	19	DY
	13	2.7	294	0.90	1.03		Black Oil	8	5	30	DY	10	4	30	DY
	14	0.4	191	0.85	0.99		Black Oil	8	4	30	DY	10	4	30	DY
	15	1.1	245				Black Oil	5	4	30	X	6	4	30	X
	16	0.8	219	0.87	1.01		Black Oil	25	13	30	X	18	7	30	X
								25	12	30					
	17	1.6	265	0.85	0.99	0.81	Black Oil	16	10	30	VDY	13	9	30	VDY
	18	1.0	228	0.87	1.01		Black Oil	21	7	30	DY	21	6	30	DY
	19	2.1	309	0.92	1.05		Black Oil	-	-	-	DY	21	10	30	DY
	20	5.3	221	0.83	0.98	0.83	Black Oil	23	11	30	X	22	10	30	X
								24	11	30					
	21	5.9	215	0.80	0.95	0.86	Black Oil	25	10	30	X	19	11	30	X
	22	5.9	215	0.78	0.94		Black Oil	22	7	30	VDY	20	6	30	VDY
	23	3.7	193	0.83	0.98	0.86	Black Oil	26	8	30	X	25	8	30	X
								27	9	30					
	24	4.0	209	0.74	0.91		Black Oil	23	5	30	VDY	22	5	30	VDY
786-3	25	0.6	123	0.83	0.98		Volatile Oil	23	11	30	X	26	12	30	X
								25	12	30					
	26	0.4	133	0.89	1.02		Volatile Oil	25	14	30	X	33	14	30	X
	667-165	27	0.8	62	1.39	1.39	Wet Gas	44	-	1	X	58	19	30	X
	28	0.5	36	1.32	1.34		Wet Gas	51	8	7	X	54	11	30	X
	29	2.7	64	1.46	1.45		Wet Gas	-	-	-	-	61	15	30	X
807-3	30	4.9	73	1.12	1.19		Wet Gas	51	7	30	X	54	6	30	X
	31	0.4	92	1.34	1.35	1.43	Wet Gas	-	-	-	-	75	8	30	X
326-3	32	0.6	66	1.98	1.83		Dry Gas	60	7	9	X	57	10	30	X
	33	0.6	60	1.86	1.74		Dry Gas	46	15	16	X	42	13	30	X
	34	0.4	72	0.90	1.03		Dry Gas	47	11	30	X	47	15	30	X
	667-47	35	4.6	25	1.44	1.43	Wet Gas	59	6	16	X	66	7	30	X
868-3	36	6.3	25	1.52	1.49	1.68	Wet/Dry Gas	-	-	-	-	80	9	30	X
	37	0.7	55	1.46	1.45	1.63	Wet/Dry Gas	69	16	8	X	82	11	30	X
	38	0.7	48	1.44	1.43	1.64	Wet/Dry Gas	61	20	12	X	85	11	30	X
	667-53A	39	2.6	21	1.13	1.20	Volatile Oil/Condensate	78	13	4	X	82	8	30	X
	40	2.6	17	1.13	1.20		Volatile Oil/Condensate	73	9	30	X	82	7	30	X
	854-3-1	41	1.7	13	2.72	2.39	2.00	Dry Gas	84	10	30	X	83	14	30
	42	1.1	9	2.72	2.39	2.00	Dry Gas	81	15	30	X	73	16	30	X
	43	2.2	8	2.72	2.39	2.00	Dry Gas	84	10	11	X	80	13	30	X
	44	1.9	7	2.17	1.98	1.93	Dry Gas	69	20	9	X	71	15	30	X

Table 2American VR_o and $PDI_{V/A}$ results. PDI results determined independently by a second operator are shown in bold italics.

Sample	Locality	Formation	Age	Av. VR_o (%)	Standard Deviation	Number of Measurements	$PDI_{V/A}$ (%)	Standard Deviation	Number of Specimens
GC-6	Bratton Branch, KY	Bedford Shale	latest Devonian	0.51	0.04	26	6	4	30
GC-14	I-64, Morehead, KY	Bedford Shale	latest Devonian	0.54	0.04	27	5	3	30
GC-8	Hannibal, MO	Hannibal Shale	earliest Carboniferous	0.49	0.05	25	6 7	3 3	30 30
GC-15	Hannibal, MO	Hannibal Shale	earliest Carboniferous	0.52	0.05	25	5 7	4 4	30 30

and pollen PDI to measured VR_o based on a large TotalEnergy dataset (Fig. 2). Spina et al. (2018) also measured acritarch PDI and correlated this to T_{max} but observed no clear correlation, a result which they attributed to the scarcity of acritarchs in some of their samples.

2. Materials and methods

2.1. Sections investigated

Forty-four productive samples were investigated for Palynomorph Darkness Index (PDI) from 15 cored well sections through the QMbr in Saudi Arabia. These ranged from immature to dry gas in terms of hydrocarbon source rock potential (Fig. 3) classified on the basis of VRE_j .

Four additional samples were collected from sections close to the Devonian/Mississippian boundary in the USA. Two of these were from the basal Mississippian Hannibal Shale Formation from its type section just outside Hannibal, Missouri, and two were collected from outcrops of the latest Devonian Bedford Shale Formation near Morehead, Kentucky.

These samples were analyzed for VR_o and PDI_A . These samples were also subjected to pyrolysis but T_{max} could not be determined due to the absence of S2 peaks.

2.2. Palynomorph darkness index (PDI)

The methodology employed for PDI measurement was that described by Clayton et al. (2017). All measurements were made on unoxidized post-HF organic residues mounted on glass slides with coverslips secured by Elvacite® non-fluorescing mounting medium. After stabilising the background illumination (RGB intensities all within the range 250–254), acritarch images were captured using a Jenoptic Gryphax® 8 MPIX digital camera mounted on a Nikon Eclipse E600 microscope with a Plan Fluor $\times 40$ objective lens. RGB intensities of representative $25 \mu m^2$ areas of the captured acritarch images were measured using the integrated Digital Colour Meter App on an Apple iMac running OS 13.6.1.

Where possible, 30 measurements of *Veryhachium/Neoveveryhachium* group acritarchs (PDI_V) were made from each sample, in order to

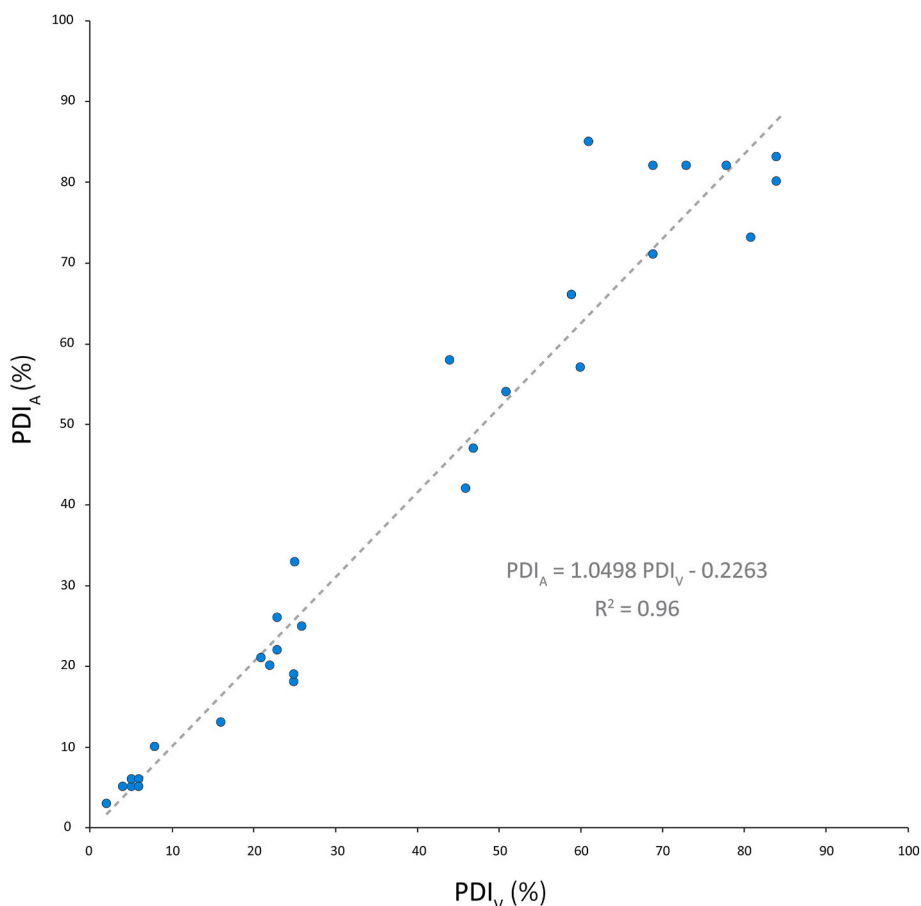


Fig. 4. Correlation of PDI_V to PDI_A from the same samples.

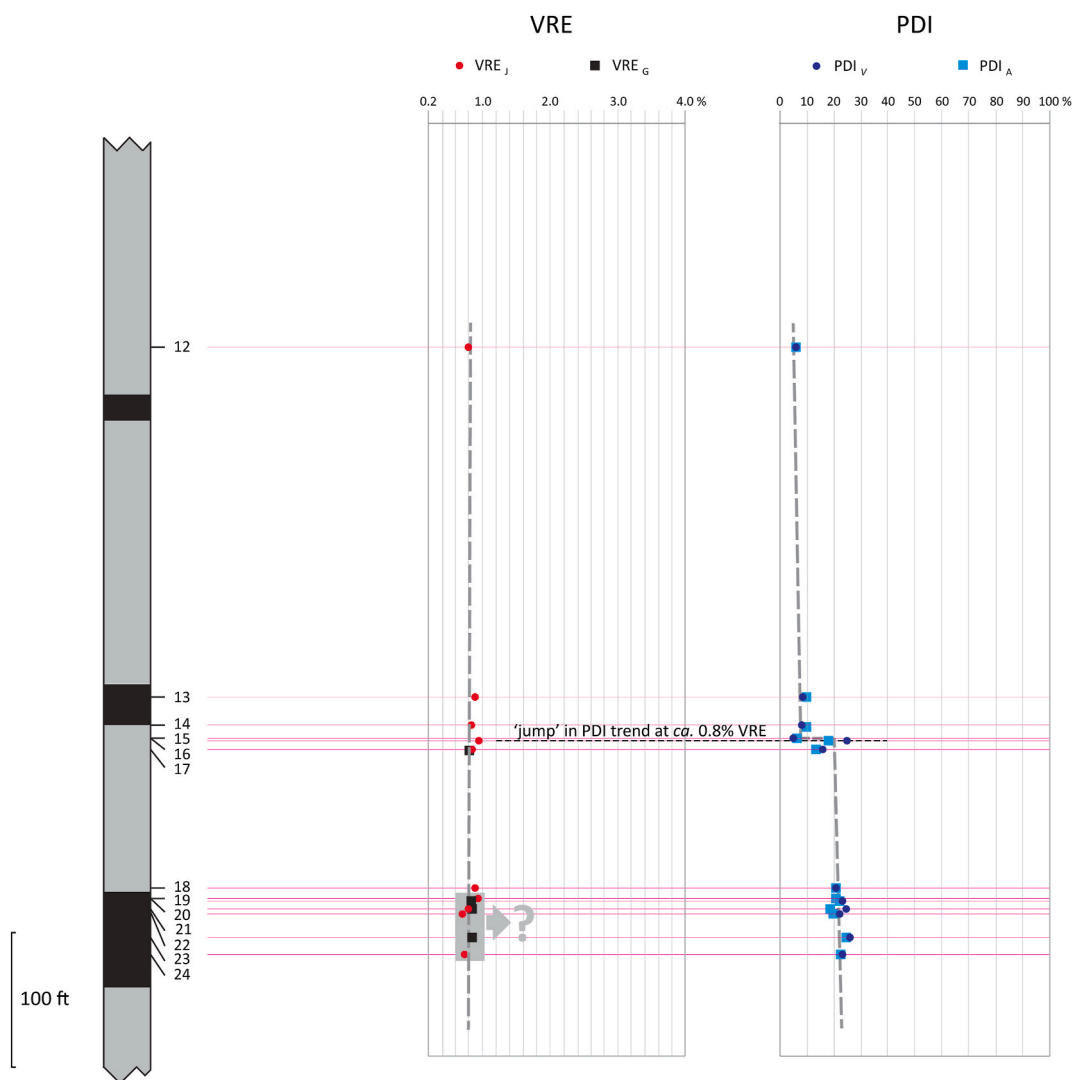


Fig. 5. VRE_J and VRE_G versus PDI_V and PDI_A in Well 488-31-1. The black intervals are 'hot' shales. The grey shading, arrow and question mark indicate VREs that may have been affected by T_{max} suppression. Red circles = VRE_J , black squares = VRE_G , dark blue circles = PDI_V , light blue squares = $PDI_{V/A}$.

minimise variation in PDI caused by wall thickness and structure. In samples where 30 specimens from this group could not be located, PDI based on 30 specimens of any acritarch (PDI_A) was determined. The PDIs of six samples were independently determined 'blind' by a second operator to assess the reproducibility of the method.

2.3. Acritarch fluorescence

Qualitative fluorescence observations were made after exposure of approximately 1 min using a Leitz Wetzlar Dialux 20 microscope with attached incident fluorescent light tube (Ploemopak 2.4), applying excitation from a violet and blue H2 Filter Block with a bandwidth of 390–490 nm. Fluorescence intensity was arbitrarily classified as bright, dull, very dull, or none. Representative examples are shown in Fig. 7, q–t and results are summarized in Tables 1 and 2.

2.4. Vitrinite reflectance

Average Vitrinite Reflectance (VR_o) of four samples was measured by Dr Cortland Eble (Kentucky Geological Survey, University of Kentucky). Rock samples were crushed and mounted in epoxy resin, then ground and polished (ASTM D2797/D2797M-21a, 2021). Vitrinite reflectance analyses were performed following the analytical protocols outlined in

ASTM D7708-23 (2023).

3. Results

3.1. Palynomorph darkness index (PDI)

All but one of the 44 QMbr samples that were productive for acritarch PDI had matching T_{max} -derived VRE data and 12 also had graptolite reflectance-derived VRE results (VRE_G). PDI_V results were obtained from 40 samples and PDI_A results were obtained from all 44 samples. All results obtained are summarized in Table 1. PDI was determined 'blind' on six samples by a second operator (Tables 1 and 2). The mean PDI results obtained were within a $\pm 2\%$ band of those determined by the first operator, confirming good reproducibility.

A strong correlation exists between of PDI_A and PDI_V from the same samples ($PDI_A = 1.0498 PDI_V - 0.2263$; $R^2 = 0.96$) (Figs. 4 and 5), especially in the less mature sections. Consequently, PDI_A is substituted for PDI_V for PDI to VRE correlation purposes with respect to the four samples from which PDI_V could not be obtained. The combined PDI_V and PDI_A results are referred to as $PDI_{V/A}$.

Correlation of acritarch $PDI_{V/A}$ to VRE_J reveals an irregular trend comprising three distinct stages (Fig. 6a). From VRE_J ca. 0.45% to VRE_J ca. 0.8%, $PDI_{V/A}$ remains very low at <10%. In the second stage from

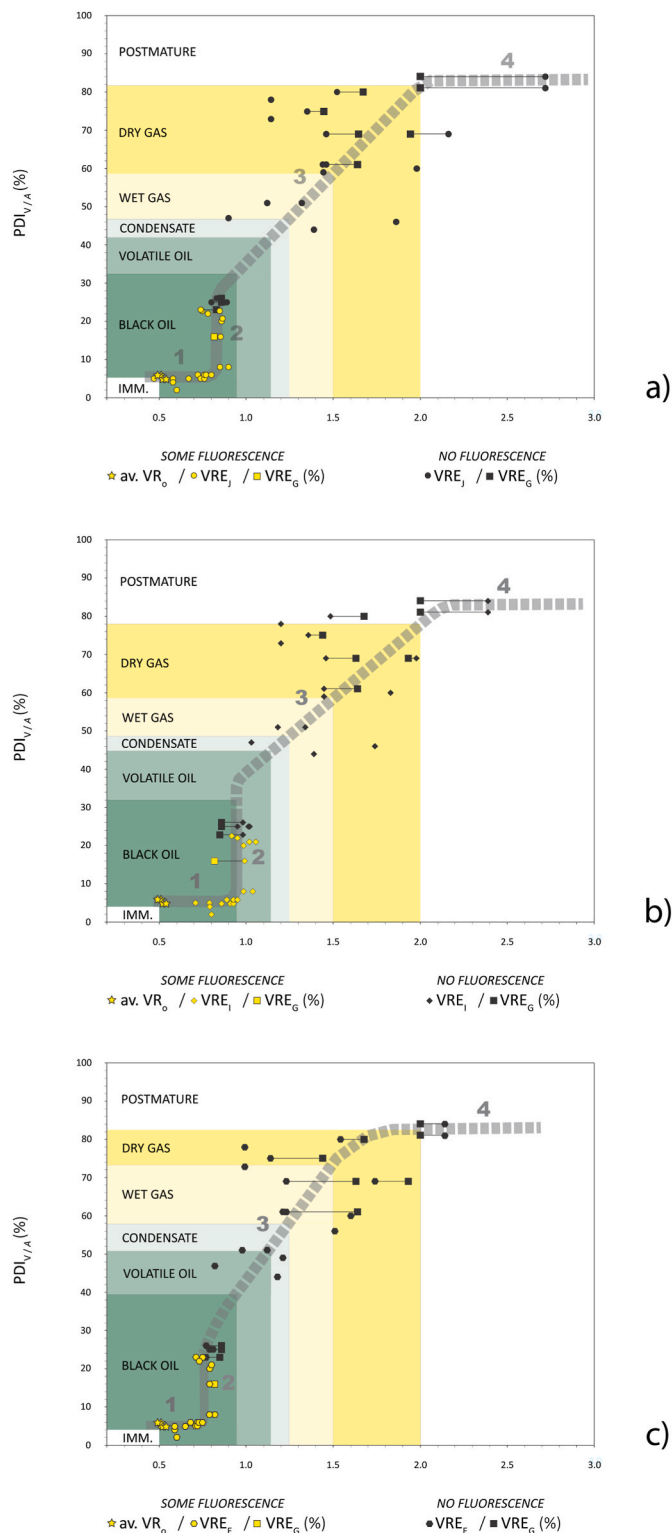


Fig. 6. Correlation of acritarch PDI ($PDI_{V/A}$) to VRE. The horizontal tie lines link VRE_G results to VRE_J , VRE_I and VRE_E results from the same sample. Fig. 6a. $PDI_{V/A}$ v. VRE_J . Fig. 6b. $PDI_{V/A}$ v. VRE_I . Fig. 6c. $PDI_{V/A}$ v. VRE_E .

VRE_J 0.8–0.9%, $PDI_{V/A}$ increases very rapidly from ca. 10% to ca. 25%. This ‘jump’ in $PDI_{V/A}$, which is not matched by any marked change in VRE_J is seen in Well 488-31-1 (Fig. 5), as well as in the overall dataset (Fig. 6a). However, T_{max} and graptolite reflectance may be suppressed in hydrogen-rich samples (Yang and Horsfield, 2020, and references therein). T_{max} may be suppressed in the lowest hot shale in Well

488-31-1 (Fig. 5, Table 1). For this reason, the VREs for this unit derived from T_{max} and graptolite reflectance values may underestimate its true maturity.

The third stage shows a gradual increase in $PDI_{V/A}$ relative to VRE_J , though this is very poorly constrained (Fig. 6a). However, there are major differences between VRE_J and VRE_G values from the same sample horizons and also significant differences in VRE_J between stratigraphically closely spaced samples in the same well sections (Table 1).

A fourth stage of the $PDI_{V/A}$ to VRE_J correlation can be postulated based on Williams et al. (1998) and on unpublished accounts of acritarch colour from postmature rocks ($VR_0/VRE > 2\%$). In this section, $PDI_{V/A}$ increases very slowly with increasing maturity, from ca. 82% to ca. 95%. The QMBr samples investigated only represent the least mature part of this stage.

Correlating $PDI_{V/A}$ to VRE_I or VRE_E rather than VRE_J (Fig. 6b and c) results in the $PDI_{V/A}$ results in the first segment shifting to the right or left respectively in the plot, i.e. suggesting that they represent a higher or lower level of maturity. The position of the $PDI_{V/A}$ ‘jump’ also shifts from VRE_J 0.8–0.9% in terms of the Jarvie conversion equation, to VRE_J 0.9–1.0% when the Inan et al. equation is used and to 0.7–0.8% using the Evenick equation.

The four latest Devonian/earliest Carboniferous samples investigated from the USA range from VR_0 0.49 – VR_0 0.52%, with $PDI_{V/A}$ 5–6%. *Veryhachium/Neoverhachium* group specimens are rare and most measurements were made on specimens of *Micrhystridium* spp. which are very similar in terms of wall thickness and diameter (Table 2).

3.2. Acritarch fluorescence

Acritarchs in the QMBr samples from PDI Stage 1 ($PDI_{V/A} < 10\%$) exhibit bright to dull fluorescence (Fig. 7), with no obvious correlation between different taxa and fluorescence intensity. Acritarchs from the four North American samples investigated (PDI_A ca. 0.5%) consistently fluoresce more brightly than acritarchs from the Saudi samples.

In PDI Stage 2 ($PDI_{V/A}$ ca. 10–25%) in the QMBr sections, there is even more variation in fluorescence intensity with subequal numbers of specimens showing bright, dull, very dull or no fluorescence in all samples. No fluorescence is seen in acritarchs from Stage 3 ($PDI_{V/A}$ ca. 25–82%) and Stage 4 ($PDI_{V/A} > 82\%$).

4. Discussion

4.1. Palynomorph darkness index (PDI)

The overall trend in acritarch PDI with increasing thermal maturity in the QMBr samples is very similar using VRE_J , VRE_I or VRE_E (Fig. 6). In the immature to main part of the black oil interval (PDI Stage 1), $PDI_{V/A}$ is $< 10\%$ and shows no clear increase with increasing maturity. In the more mature part of the Black Oil Window or at its boundary with the Volatile Oil Window (depending on whether VRE_J , VRE_I or VRE_E is used), $PDI_{V/A}$ increases very rapidly compared to VRE, from ca. 10% – ca. 25% (PDI Stage 2). This PDI ‘jump’ almost certainly corresponds to the rapid change of acritarch colour in the middle of the Oil Window noted by Williams et al. (1998).

Correlation of miospore PDI to vitrinite reflectance (VR_0) by Buratti et al. (2024) shows a gradual increase in PDI relative to VR_0 from 0.2% to 0.7%, at which point there is a distinct ‘jump’ in PDI (Fig. 2). PDI then returns to a gradual increase from VR_0 0.7–2.0%, from which point it only increases very slowly to at least VR_0 2%. Yule et al. (1998) noted a rapid change in quantitative spore colour in the interval VR_0 0.6–1.04%, with the greatest range of colour in a single sample also recorded within this maturity interval. Yule et al. (2000) described an increase in the rate of change in colour beginning at ca. VR_0 0.8% in naturally matured Carboniferous miospores. Based on FTIR investigation of the same samples, these authors concluded that this was associated with the loss of aliphatic groups to form hydrocarbons. Ujjié (2001) recorded

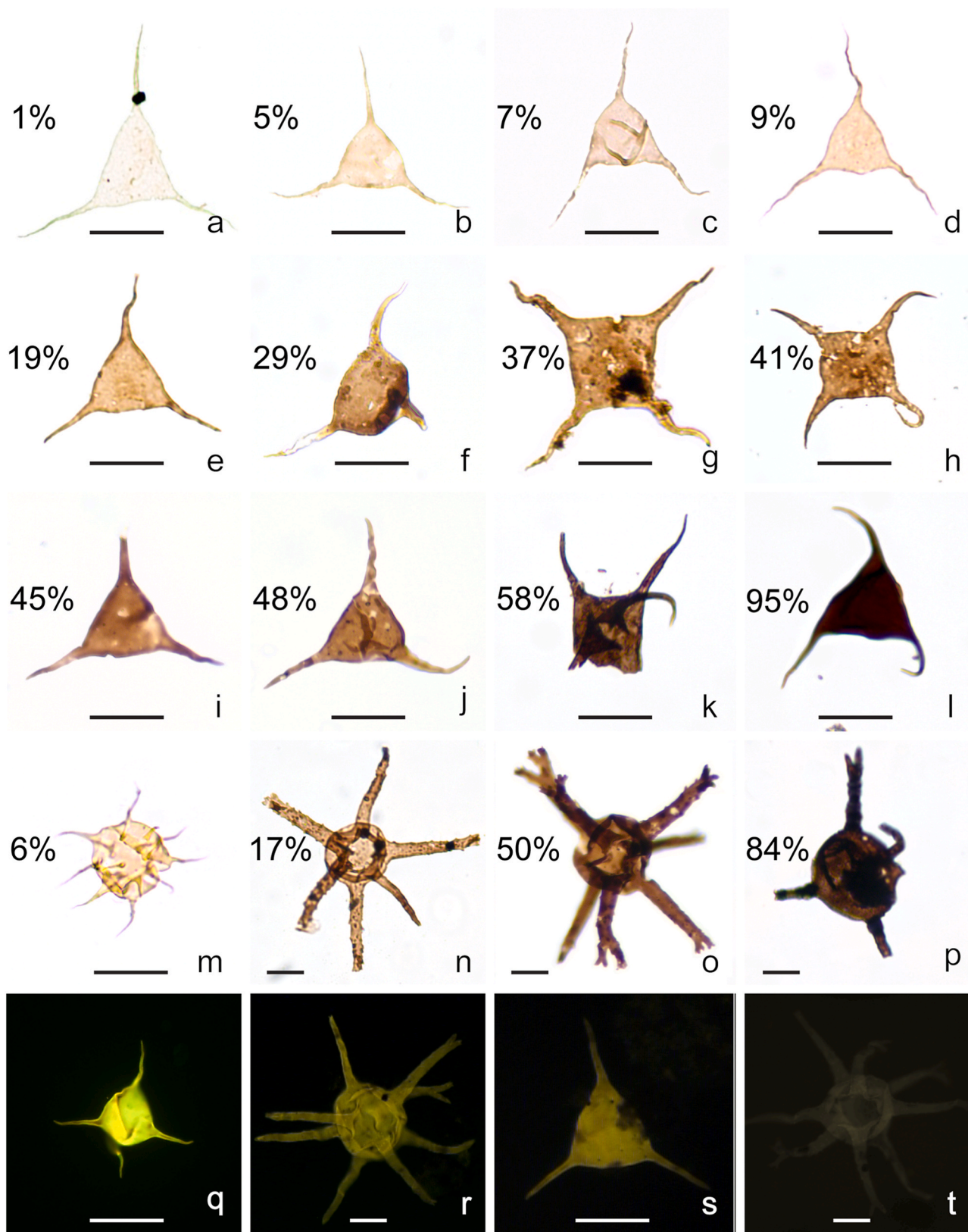


Fig. 7. A – l. Representative specimens from the *Veryhachium/Neoveryhachium* group of acritarchs illustrating increasing PDI (shown to the left of each specimen). m – p. other acritarchs. q – t. acritarchs exhibiting bright fluorescence (q), dull fluorescence (r, s) and very dull fluorescence (t). Scale bars are 25 μm .

accelerated increase of stTAI of Neogene pollen between VR_0 0.5% and 0.6%, corresponding to the, “threshold zone of oil generation.”

Our QMbr results and the independent studies discussed above suggest that there is a rapid increase in the rate of palynomorph darkening within the maturity range 0.5–1.04% VR_0 but this may occur at different maturity levels in different palynomorph groups and with different kerogen compositions. However, the basal hot shale in Well 488-31-1 is more organic rich than the section above, with higher TOC and HI values (Table 1). In other wells with continuously measured TOC, HI and T_{max} data, there is clear evidence of T_{max} (and derived VRE) suppression in this unit but this cannot be conclusively established in Well 488-31-1 due to the lack of data from the interval separating the two hot shales. Consequently, there is a strong possibility that, in our study, suppression of T_{max} has modified the position of the PDI ‘jump’ on the VRE axis (Fig. 6 a, b, c), by underestimating the level of maturity at which it occurs, thereby exaggerating its apparent magnitude. Further research is planned on other wells that span this maturity interval in order to elucidate this relationship.

Within PDI Stage 3 ($\text{PDI}_{\text{V/A}}$ ca. 25–82%) of the present investigation, PDI clearly increases with VRE_J , VRE_I and VRE_G but with considerable scatter and consequent weak correlation. This is in marked contrast to the strong correlation between PDI and VR_0 recorded by Buratti et al. (2024) through the same maturity interval. In contrast with the present acritarch-based PDI results, Buratti et al. (2024) published PDI results obtained exclusively from pollen and spores. Differences in chemical composition of the walls of these palynomorph groups are probably too minor to have significantly affected their optical properties. As a consequence, the scatter in the acritarch PDI v. VRE data is most likely explained by the correlation to pyrolysis-based VREs in the present study compared to the correlation to (measured) VR_0 of Buratti et al. (2024). This interpretation is supported by Evenick’s (2021) conclusion that, “ R_0 is a robust thermal maturity indicator, but there is no definitive correlation between pyrolysis-based thermal maturity indicators and R_0 ” (Note, $R_0 = \text{VR}_0$).

Only two samples in the present study are assigned to PDI Stage 4 ($\text{PDI}_{\text{V/A}} > 82\%$) within which acritarchs are more-or-less black and there is little increase in $\text{PDI}_{\text{V/A}}$ with increasing VRE_J . This maturity interval is much better represented in terms of spore and pollen PDI v. VR_0 (Buratti et al., 2024), though it should be noted that T_{max} -based VREs are inaccurate at this level of maturity and, due to increased birefractance, VR_{max} is a more appropriate indicator of maturity than VR_0 .

In discussing acritarchs and prasinophytes from the Lower Cambrian Laeså Formation on Bornholm, Denmark, Moczyłowska and Vidal (1992) described darker acritarchs from phosphorite bearing units than from associated shales and mudstones. They tentatively suggested that this could have been caused by natural radioactive decay of radiogenic elements including uranium concentrated in the phosphorites. There is no evidence of any comparable increase in acritarch PDI in samples from the more organic (and presumably uranium) rich units in the QMbr.

4.2. Acritarch fluorescence

Acritarch fluorescence intensity is apparently suppressed in samples from the QMbr, with duller fluorescence in PDI Stage 1 than in samples of similar maturity from the USA. Total extinction of fluorescence in the QMbr occurs within the VRE range 0.8–1.1% (depending on which VRE is used). Fluorescence of oil shows and fluid inclusions usually disappears at the boundary between the volatile oil and condensate windows (VRE 1.2%). Reviewing previous work, Hartkopf-Fröder et al. (2015) concluded that visible fluorescence of sporinite is generally extinguished at VR_0 1.2–1.3%.

In terms of the coal and organic petrology classification of organic matter, acritarchs belong to the liptinite (formerly exinite) maceral subgroup, together with all other palynomorphs (Pickel et al., 2017). Except for Sorchi et al. (2020), very few publications discuss fluorescence of acritarchs but there are numerous published accounts of the

modification of liptinite fluorescence. Of these, the most significant is Zheng et al. (2021) who conducted a comprehensive investigation of Baltoscandian Paleozoic alum shales. These authors reported a reduction of up to 95.6% in liptinite fluorescence relative intensity associated with an increase in U content from 29 to 401 ppm. They also noted that solid bitumen reflectance appeared to be, “significantly elevated in micro scale proximity to the U-containing minerals” and that there was a heterogenous distribution of U-containing minerals within the samples studied. If irradiation from a comparable heterogenous distribution of U-containing minerals in the QMbr has affected acritarch fluorescence on a similar micro scale, this could have contributed to the wide variation in fluorescence intensity recorded.

5. Conclusions

The *Veryhachium/Neoverhachium* group of acritarchs is the most suitable group for Palynomorph Darkness Index (PDI) determination, but measurements based on all acritarchs can be substituted, though inclusion of large, thick-walled forms in samples (where these are common) can skew the mean towards the higher (darker) end of the PDI scale.

As thermal maturity increases, acritarch Palynomorph Darkness Index (PDI) increases in an irregular manner compared to pyrolysis derived Vitrinite Reflectance Equivalents (VREs). With regard to the VRE/PDI correlation trendline, four distinct stages can be recognized. In the least mature of these (PDI Stage 1) PDI is <10% and acritarchs fluoresce. In the second stage from VRE_J 0.8–0.9%, $\text{PDI}_{\text{V/A}}$ increases very rapidly from ca. 10% to ca. 25%. The third stage shows a gradual increase in PDI relative to VRE, though this is poorly constrained. In the fourth stage, PDI increases very slowly with increasing maturity, from ca. 82% to ca. 95%. The Qusaiba Member samples investigated represent only the least mature part of this stage.

Acritarch fluorescence is less intense and is extinguished at a lower level of thermal maturity (VRE ca. 0.95% and PDI ca. 25%) in the Qusaiba samples than has been reported from other investigations.

CRedit authorship contribution statement

Geoff Clayton: Writing – original draft, Project administration, Methodology, Investigation, Formal analysis, Data curation, Conceptualization. **Marco Vecoli:** Writing – review & editing, Writing – original draft, Project administration, Methodology, Investigation, Formal analysis, Data curation, Conceptualization. **Pan Luo:** Writing – review & editing, Writing – original draft, Project administration, Methodology, Investigation, Formal analysis, Data curation, Conceptualization. **Robbie Goodhue:** Writing – review & editing, Writing – original draft, Resources, Methodology, Investigation, Formal analysis, Conceptualization. **Charles Wellman:** Writing – review & editing, Project administration, Methodology, Investigation, Formal analysis.

Declaration of competing interest

The authors declare that they have no known competing financial interests or personal relationships that could have appeared to influence the work reported in this paper.

Data availability

Data will be made available on request.

Acknowledgements

We wish to thank Dr Amalia Spina and Dr Nicoletta Buratti for their helpful advice and generous access to their unpublished data during the course of this project. This research did not receive any specific grant from funding agencies in the public, commercial, or not-for-profit

sectors. This is a contribution to the Saudi Aramco-CIMP Special Project 'Palaeozoic Palynology of the Arabian Plate'.

References

- ASTM D2797/D2797M-21a, 2021. Standard practice for preparing coal samples for microscopical analysis by reflected light. ASTM International, West Conshohocken, PA, USA.
- ASTM D7708-23, 2023. Standard test method for microscopical determination of the reflectance of vitrinite dispersed in sedimentary rocks. ASTM International, West Conshohocken, PA, USA.
- Boukhamsin, H., Vecoli, M., Breuer, P., Ertug, K., 2013. High-resolution integrated palynological and graptolite biozonation in the early Silurian of the Arabian Plate. AAPG-TPS 46th Annual Meeting, San Francisco, California, USA, October 20–24, 2013, Abstracts and Program 52.
- Buratti, N., De Luca, R., Garuti, L., Sorci, A., Spina, A., Clayton, G., 2024. Thermal maturity evaluation on mildly artificially oxidized sporomorphs: a comprehensive calibration of palynomorph darkness index (PDI) with vitrinite reflectance. *Mar. Petrol. Geol.* <https://doi.org/10.1016/j.marpetgeo.2023.106672>, 2024.
- Cheshire, S., Craddock, P.R., Xu, G., Sauerer, B., Pomerantz, A.E., McCormick, D., Abdallah, W., 2017. Assessing thermal maturity beyond the reaches of vitrinite reflectance and Rock-Eval pyrolysis: a case study from the Silurian Qusaiba formation. *Int. J. Coal Geol.* 180, 29–45.
- Clayton, G., Goodhue, R., Abdelbagi, S., Vecoli, M., 2017. Correlation of Palynomorph Darkness Index and vitrinite reflectance in a submature Carboniferous well section in northern Saudi Arabia. (2017). *Rev. Micropaleontol.* 60 (3), 411–416.
- Cole, G.A., 1994. Graptolite-chitinozoan reflectance and its relationship to other geochemical maturity indicators in the Silurian Qusaiba Shale, Saudi Arabia. *Energy Fuel* 8 (6), 1443–1459.
- Cole, G.A., Abu-Ali, M.A., Aoudeh, S.M., Carrigan, W.J., Chen, H.H., Colling, E.L., et al., 1994. Organic geochemistry of the Paleozoic petroleum system of Saudi Arabia. *Energy Fuel* 8 (6), 1425–1442.
- Collins, A., 1990. The 1–10 Spore Colour Index (SCI) scale: a universally applicable colour maturation scale, based on graded, picked palynomorphs. *Meded. Rijks Geol. Dienst* 45, 39–47.
- Duggan, M.B., Clayton, G., 2008. Colour change in the acritarch *Veryhachium* as an indicator of thermal maturity. *GeoArabia* 13 (3), 125–136.
- Ertug, K., Vecoli, M., Inan, S., 2019. Palynofacies, paleoenvironment and thermal maturity of early silurian shales in Saudi Arabia (Qusaiba member of Qalibah Formation). *Rev. Palaeobot. Palynol.* 270, 8–18.
- Evenick, J.C., 2021. Examining the relationship between Tmax and vitrinite reflectance: an empirical comparison between thermal maturity indicators. *J. Nat. Gas Sci. Eng.* 91 (2021), 103946.
- Goodarzi, F., Fowler, M.G., Bustin, M., McKirdy, D.M., Trudinger, A., 1992. Thermal maturity of Lower Palaeozoic sediments as determined by the optical properties of marine-derived organic matter. In: Schilowski, M., Goilubic, S., Kimberley, M.M., McKirdy, D.M. (Eds.), *Early Organic Evolution*. Springer Verlag, pp. 279–295.
- Goodhue, R., Clayton, G., 2010. Palynomorph Darkness Index (PDI) – a new technique for assessing thermal maturity. *Palynology* 34 (2), 147–156.
- Hartkopf-Froder, C., Königshof, P., Littke, R., Schwarzbauer, J., 2015. Optical thermal maturity parameters and organic geochemical alteration at low grade diagenesis to anchimetamorphism: a review. *Int. J. Coal Geol.* 150–151, 74–119.
- Hayton, S., Rees, A.J., Vecoli, M., 2017. A punctuated Late Ordovician and early Silurian deglaciation and transgression: evidence from the subsurface of northern Saudi Arabia. *AAPG (Am. Assoc. Pet. Geol.) Bull.* 101 (6), 863–886.
- Inan, S., Goodarzi, F., Mumm, A.S., Arouri, K., Qathami, S., Ardakani, O.H., Inan, T., Tuwailib, A.A., 2016. The silurian Qusaiba hot shales of Saudi Arabia: an integrated assessment of thermal maturity. *Int. J. Coal Geol.* 159, 107–119.
- Jarvie, D., Claxton, B., Henk, F., Breyer, J., 2001. Oil and Shale Gas from the Barnett Shale, Ft. Worth Basin, Texas: AAPG National Convention, June 3–6, 2001. AAPG Bulletin, Denver, CO, p. A100, 85 (Suppl).
- Loydell, D.K., Butcher, A., Fryda, J., Luning, S., Fowler, M., 2009. Lower Silurian "hot shales" in Jordan: a new depositional model. *J. Petrol. Geol.* 32, 261–270.
- Loydell, D.K., Butcher, A., Fryda, J., 2013. The middle Rhuddanian (lower Silurian) 'hot' shale of North Africa and Arabia: an atypical hydrocarbon source rock. *Palaeogeogr. Palaeoclimatol. Palaeoecol.* 386, 233–256.
- Lüning, S., Craig, J., Loydell, D.K., Storch, P., Fitches, B., 2000. Lower Silurian 'hot shales' in North Africa and Arabia: regional distribution and depositional model. *Earth Sci. Rev.* 49, 121–200.
- Marshall, J.E.A., 1991. Quantitative spore colour. *J. Geol. Soc.* 148, 223–233.
- McPhilemy, B., 1998. The value of fluorescence microscopy in routine palynofacies analysis: Lower Carboniferous successions from counties Armagh and Roscommon, Ireland. *Rev. Palaeobot. Palynol.* 56, 345–359.
- Milton, J.A., 1993. The application of quantitative spore colour measurement to thermal maturity studies. Unpublished Ph.D. Dissertation, University of Southampton, 312 pp.
- Moczyłowska, M., Vidal, G., 1992. Phytoplankton from the lower cambrian lesa Formation on Bornholm, Denmark: biostratigraphy and palaeoenvironmental constraints. *Geol. Mag.* 129, 17–40.
- Petersen, H.L., Schovsbo, N.H., Nielsen, A.T., 2013. Reflectance measurements of zooclasts and solid bitumen in Lower Paleozoic shales, southern Scandinavia: correlation to vitrinite reflectance. *Int. J. Coal Geol.* 114, 1–18.
- Pickel, W., Kus, J., Flores, D., Kalaitzidis, S., Christianis, K., Cardott, B.J., Niz-Kennan, M., Rodrigues, S., Hentschel, A., Hamor-Vido, M., Crosdale, P., Wagner, N., 2017. Classification of liptinite-iccp system 1994. *Int. J. Coal Geol.* 169, 40–61. ICCP.
- Sorci, A., Cirilli, S., Clayton, G., Corrado, S., Hints, O., Goodhue, R., Spina, A., 2020. Palynomorph optical analyses for thermal maturity assessment of Upper Ordovician (Katian-Hirnantian) rocks from Southern Estonia. *Mar. Petrol. Geol.* 120, 104574.
- Spina, A., Vecoli, M., Riboulleau, A., Clayton, G., Cirilli, S., Di Michele, A., Marcoguiseppe, A., Rettori, R., Sassi, P., Servais, T., Riquier, L., 2018. Application of Palynomorph Darkness Index to assess the thermal maturity of palynomorphs: a case study from North Africa. *Int. J. Coal Geol.* 188, 64–78.
- Spina, A., Cirilli, S., Sorci, A., Schito, A., Clayton, G., Corrado, S., Fernandes, P., Galasso, F., Montes, G., Pereira, Z., Rashidi, M., Rettori, R., 2021. Assessing thermal maturity through a multi-proxy approach: a case study from the permian faraghan formation (zagros basin, southwest Iran). *Geosciences* 11, 484.
- Staplin, F.L., 1969. Sedimentary organic matter, organic metamorphism, and oil and gas occurrence. *Bull. Can. Petrol. Geol.* 17, 47–66.
- Strullu-Derrien, C., Bernard, S., Spencer, A.R.T., Remusat, L., Kenrick, P., Derrien, D., 2019. On the structure and chemistry of the earliest woody plant. *Palaeontology* 62 (6), 1015–1026.
- Teichmüller, M., Wolf, M., 1977. Application of fluorescence microscopy in coal petrology and oil exploration. *J. Microsc.* 109, 49–73.
- Tricker, P.M., Marshall, J.E.A., Badman, T.D., 1992. Chitinozoan reflectance: a Lower Paleozoic thermal maturity indicator. *Mar. Petrol. Geol.* 9, 302–307.
- Ujjié, Y., 2001. Brightness of pollen as an indicator of thermal alteration by means of a computer-driven image processor: statistical thermal alteration index (STAD). *Org. Geochem.* 32, 127–141.
- Vecoli, M., Delabroye, A., Spina, A., Hints, O., 2011. Cryptospore assemblages from upper ordovician (Katian-Hirnantian) strata of anticosti island, québec, Canada, and Estonia: palaeophytogeographic and palaeoclimatic implications. *Rev. Palaeobot. Palynol.* 166 (1–2), 76–93.
- Van Gijzel, P., 1967. Palynology and fluorescence microscopy. *Rev. Palaeobot. Palynol.* 2, 49–79.
- Wellman, C.H., Breuer, P., Miller, M.A., Owens, B., Al-Hajri, S., 2015. Palaeozoic palynostratigraphy of the Arabian Plate [a joint project between Saudi Aramco and the Commission Internationale de Microflore du Paléozoïque (CIMP)]. *Rev. Palaeobot. Palynol.* 212, 1–2.
- Williams, M., Zalasiewicz, J.A., Boukhamsin, H., Cesari, C., 2016. Early Silurian (Llandovery) graptolite assemblages of Saudi Arabia: biozonation, palaeoenvironmental significance and biogeography. *Geol. Q.* 60, 3–25.
- Williams, S.H., Burden, E.T., Mukhopadhyay, P.K., 1998. Thermal maturity and burial history of Paleozoic rocks in western Newfoundland. *Can. J. Earth Sci.* 35, 1307–1322.
- Yang, S., Horsfield, B., 2020. Critical review of the uncertainty of Tmax in revealing the thermal maturity of organic matter in sedimentary rocks. *Int. J. Coal Geol.* 225, 103500.
- Yule, B.L., Roberts, S., Marshall, J.E.A., Milton, J.A., 1998. Quantitative spore colour measurement using colour image analysis. *Org. Geochem.* 28 (3/4), 139–149.
- Yule, B.L., Roberts, S., Marshall, J.E.A., 2000. The thermal evolution of sporopollenin. *Org. Geochem.* 31, 859–870.
- Zheng, X., Schovsbo, N.H., Bian, L., Luo, Q., Zhong, N., Rudra, A., Goodarzi, F., Sanei, H., 2021. Alteration of organic macerals by uranium irradiation in lower Paleozoic marine shales. *Int. J. Coal Geol.* 239, 103713.